



Synthesis, Spectral and Thermal Characterization of Selected Metal Complexes Containing Schiff Base Ligands with Antimicrobial Activities

Farhana Afsan¹, Sadia Afrin Dalia¹, Saddam Hossain², Shaheen Sarker³
and Kudrat-E-Zahan^{1*}

¹Department of Chemistry, Rajshahi University, Rajshahi, Bangladesh.

²Department of Chemistry, Begum Rokeya University, Rangpur, Bangladesh.

³Department of Industrial Science and Technology, University of Pahang, Malaysia.

Authors' contributions

This work was carried out in collaboration between all authors. Author KEZ designed the study. Authors FA, SAD and SH did the study, laboratory work and wrote the first draft of the manuscript. Author SS managed the TGA/DTG analysis. All authors read and approved the final manuscript.

Article Information

DOI: 10.9734/AJOCS/2018/40913

Editor(s):

(1) Ling Bing Kong, School of Materials Science and Engineering, Nanyang Technological University, Singapore.

(2) Wenzhong Shen, Professor, Institute of Coal Chemistry, Chinese Academy of Sciences, China.

Reviewers:

(1) Nadia Sabry El-Gohary, Mansoura University, Egypt.

(2) Erik de Leeuw, University of Maryland Baltimore School of Medicine, USA.

Complete Peer review History: <http://prh.sdiarticle3.com/review-history/24702>

Original Research Article

Received 25th February 2018
Accepted 8th May 2018
Published 21st May 2018

ABSTRACT

Selected metal complexes of Ni (II), Zn(II), Mn(II), Sn(II), Co(II) and Cd(II) ions were synthesized with three different synthesized Schiff base ligands. The ligands and metal complexes were isolated in the solid state from the reaction medium and characterized by molar conductivity measurement, magnetic susceptibility, Infrared, electronic spectral, thermal analysis and some physical measurements. The overall reactions were monitored by TLC analysis. Molar conductance study has shown that all the complexes were non-electrolytic in nature. FTIR studies suggested that Schiff bases act as deprotonated bidentate ligands and metal ions are attached with the ligands through N, O/S coordinating sites during complexation reaction. Magnetic susceptibility data coupled with electronic spectra revealed that Zn(II), Mn(II), Sn(II), and Cd(II) complexes have tetrahedral, Ni(II) complexes have a square planer and Co(II) complexes have octahedral geometry. Thermal analysis

*Corresponding author: E-mail: kudrat.chem@ru.ac.bd;

(TGA and DTG) data showed the possible degradation pathway of the complexes and also indicated that most of the complexes were thermally stable up to 200°C. The Schiff bases and their metal complexes have been found moderate to strong antimicrobial activity.

Keywords: Schiff base; thiosemicarbazide; TGA; DTG; antimicrobial activity.

1. INTRODUCTION

Multidentate ligands are extensively used for the preparation of metal complexes with interesting properties [1-5]. Among these ligands, Schiff bases containing nitrogen and phenolic oxygen donor atoms are of considerable interest due to their potential application in catalysis, medicine and material science [6-9]. Transition metal complexes of these ligands exhibit varying configurations, structural liability and sensitivity to molecular environments. The central metal ions in these complexes act as active sites for pharmacological agent. This feature is employed for modelling active sites in biological systems.

Thiosemicarbazones obtained by the condensation reaction of thiosemicarbazide and different aldehydes or ketones are important chemicals due to their broad profile of pharmacological activity. The transition metal complexes of thiosemicarbazone are also played important role in antimicrobial, antitumour and anticancer activities.

Therefore, in view of our interest in the synthesis of new Schiff base complexes, which might find application as pharmacological and as luminescence probes, we have synthesized and characterized new transition metal complexes of Schiff bases formed by the condensation reaction of different aldehydes and amino acids. The results of our studies are presented in this article.

2. EXPERIMENTAL

2.1 Materials and Methods

All chemicals and solvents used were of the Analar grade. All metal(II) salts were used as chloride and sulphate. The solvents such as Ethanol, methanol, chloroform, Diethyl ether, petroleum ether, DMSO (dimethyl sulfoxide) and acetonitrile were purified by standard procedure. The melting point or the decomposition temperature of all the prepared ligand and metal complexes were observed in an electrothermal

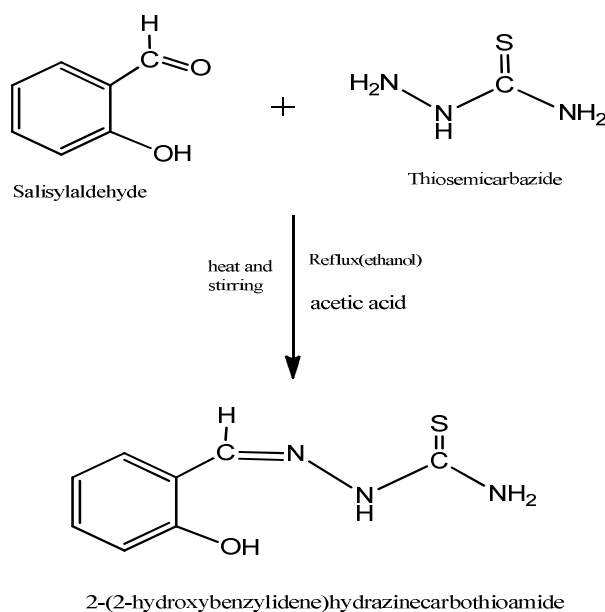
melting point apparatus model No. AZ6512. Vibrational spectra (IR) were recorded with a NICOLET 310, FTIR spectrophotometer, Belgium, in the range 4000-225 cm^{-1} with a KBr disc as a reference. UV-Visible spectra of the complexes in DMSO ($0.5 \times 10^{-3} \text{M}$) were recorded in the region 200-800 nm on a Thermolectron Nicolet evolution 300 UV-Visible spectrophotometer. The SHERWOOD SCIENTIFIC Magnetic Susceptibility Balance that following the Gouy Method were used to measure the magnetic moment of the solid complexes. The electrical conductance measurements were made at room temperature in freshly prepared aqueous solution (10^{-3}M) and in DMSO using a WPACM35 conductivity meter and a dip-cell with a platinum electrode. The thermogravimetric analyses (TGA) were performed on Perkin Elmer Simultaneous Thermal Analyzer, STA-8000. The purity of the ligand and metal complexes were tested by Thin Layer Chromatography (TLC).

2.1 Synthesis of Schiff base LIGAND $\text{C}_8\text{H}_9\text{ON}_3\text{S}$ (L^1)

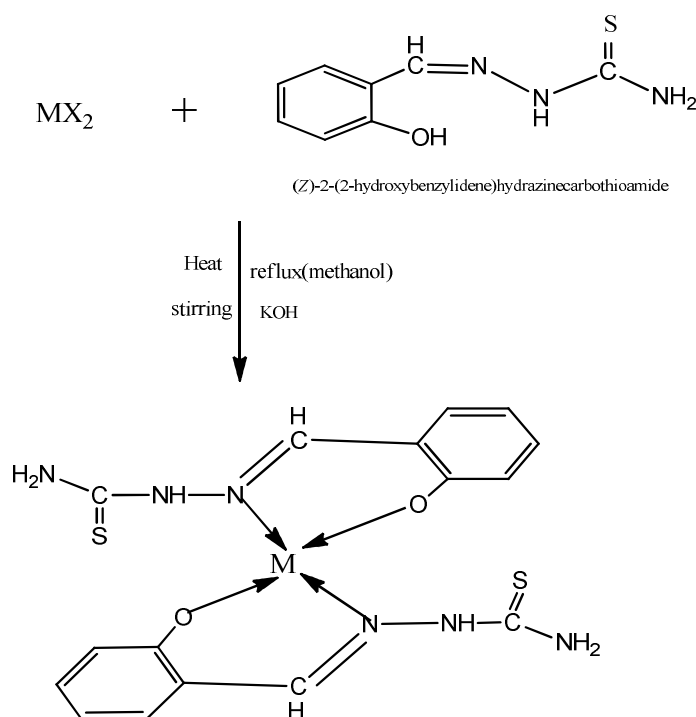
The ligand was prepared by condensation reaction of 20 mmoles of salicylaldehyde (1.048 ml) with 20 mmole (1.82 gm) of thiosemicarbazide in a clean round-bottomed flask. Salicylaldehyde was dissolved in 20ml ethanol and thiosemicarbazide was dissolved in hot ethanol with water. The solutions were mixed and refluxed for 3-4 hours. On cooling off-white colored product was formed which was washed with ethanol, acetone, and diethyl ether and dried in vacuum desiccators over anhydrous CaCl_2 . The purity of ligand was tested by TLC using different solvents. The product was found to be soluble in methanol, chloroform and DMSO. It provided 80% yield at 34°C. The target Schiff base was synthesized according to Schema-1.

2.3 Synthesis of Metal Complexes Using Schiff Base Ligand $\text{C}_{14}\text{H}_{11}\text{O}_3\text{N}$ (L^1)

The synthesized complexes have the general formula $[\text{M}(\text{SB})_2]$; where M= Zn(II), Ni(II) and



Schema 1. Synthetic pathway of Schiff base ligand C₁₄H₁₁O₃N (L¹)



Schema 2: Synthetic pathway of Schiff Base Ligand (L²) Metal Complexes, with M=Zn(II), Ni(II), Mn(II), and Sn(II) ions and X=Cl⁻, SO₄²⁻ ions

Mn(II) and SB = synthesized Schiff base ligand (Schema 2). During complexation reaction, 15 ml methanolic solution of Zinc(II) sulphate (0.2875 g, 1 mmol)/ Ni(II) chloride hexahydrate (0.238 g, 1mmol)/ Manganese(II) chloride tetrahydrate (0.198 g, 1 mmol) was taken in a two-necked round bottom flask and kept on a magnetic

stirring. A methanolic solution (20 mL) of prepared Schiff base ligand (0.390 g, 2 mmol) was added dropwise and a methanolic solution (10 mL) of KOH (0.1122 g, 1 mmol) was added slowly then the resultant mixture was heated with constant stirring on a magnetic stirrer for 4-5 hours. On cooling colored solid product was

formed which was washed with methanol, acetone, ether and dried in vacuum over anhydrous CaCl_2 . The reaction was monitored by TLC using petroleum ether, toluene, ethyl acetate and methanol as solvent. The common structure of metal complexes has been shown in Schema-1 and individual expected structures of the complexes are shown as supplementary materials.

2.4 Synthesis of Schiff Base LIGAND $\text{C}_{14}\text{H}_{11}\text{O}_3\text{N}$ (L^2)

4-hydroxy benzaldehyde (2.44 g, 20 mmol) dissolved in absolute ethanol (20-25 mL) was added dropwise to a constant stirring solution of 4-aminobenzoic acid (2.76 g, 20 mmol) in 30 mL ethanol and 2 mL of conc. glacial acetic acid was added slowly. Then the mixture was refluxed for (4-5)h. On cooling, a solid yellow product was formed which was filtered, washed with ethanol and diethyl ether and dried in vacuum over anhydrous CaCl_2 . The reaction was monitored by TLC using petroleum ether, ethyl acetate, toluene and methanol solvents. The product was found to be soluble in methanol, chloroform and DMSO. It provided 65% yield at 34°C . The target Schiff base was synthesized according to Schema-3.

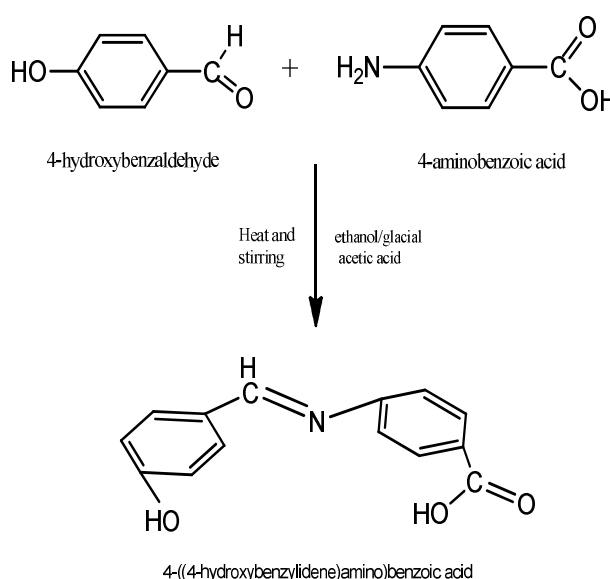
2.5 Synthesis of Metal Complex Using Schiff Base Ligand (L^2)

The complex was prepared in 1:2 molar ratio (metal: ligand). A methanolic solution (20 mL) of

cobalt(II) chloride hexahydrate (0.24 g, 1 mmol) was taken in a two-necked round bottom flask and kept on magnetic stirring and a methanolic solution (20 mL) of prepared Schiff base ligand (0.483 g, 2 mol) was added dropwise and stirred with heating for 4-5h. On cooling, the precipitate was formed which was filtered, washed with ethanol, acetone, and diethyl ether and dried in vacuum desiccators over anhydrous CaCl_2 . The purity of complex was tested by TLC using different solvents. The complex was soluble in DMSO with heat. The proposed structure of the complex is shown in Schema-4.

2.6 Synthesis of Schiff Base Ligand $\text{C}_9\text{H}_{11}\text{N}_3\text{OS}$ (L^3)

To a stirring solution of thiosemicarbazide (0.91 gm, 10 mmol) dissolved in 20 mL of ethanol with water, a solution of Anisaldehyde (1.22 mL, 10 mmol) in 10 mL ethanol was added dropwise. After sometime 2ml of glacial acetic acid was added with the reaction mixture and the solution was refluxed for 5-6 h and allowed to cool overnight in room temperature. The off-white product was filtered washed several times with ethanol and finally with diethyl ether and dried in vacuum over anhydrous CaCl_2 . The reaction was monitored by TLC using petroleum ether, ethyl acetate, toluene and methanol solvents. The product was found to be soluble in methanol, DMF and DMSO. It provided 62% yield. The Schiff base was synthesized according to Schema-5.



Schema 3. Synthetic pathway of Schiff base ligand $\text{C}_{14}\text{H}_{11}\text{O}_3\text{N}$ (L^2)

stirred with heating for 4-5 h. On cooling, the precipitate was formed which was filtered, washed with ethanol, acetone, and diethyl ether and dried in vacuum desiccators over anhydrous CaCl_2 . The reaction was monitored by TLC using different solvents. The complex was soluble in DMSO with heat. The proposed structure of the complex is shown in Scheme 6.

3. CHARACTERIZATION OF THE LIGANDS AND COMPLEXES

The structures of the complexes were characterized by melting point, conductivity measurements, magnetic susceptibility, IR spectra and UV visible spectra [10] analysis. The purity of the ligands and metal complexes were monitored by Thin Layer Chromatography (TLC). The ligands and complexes are characterized below by these methods.

3.1 Melting Point

Melting point gives an approximate idea about the nature of the complexes and can suggest whether it is covalent or ionic [11]. The melting point of all the synthesized ligands and complexes are shown in Table 1.

3.2 Conductivity

The molar conductivities were obtained using the formula

$$\Lambda = \frac{1000}{C} \times \text{Cell constant} \times \text{Observed conductivity}, \quad (1)$$

Where, Λ =molar conductance, C = concentration. The molar conductance is calculated from the measured specific conductance at room temperature by using the above equation. The experimental results are shown in Table 2.

From the table data, it is showed that all the complexes are non-electrolyte.

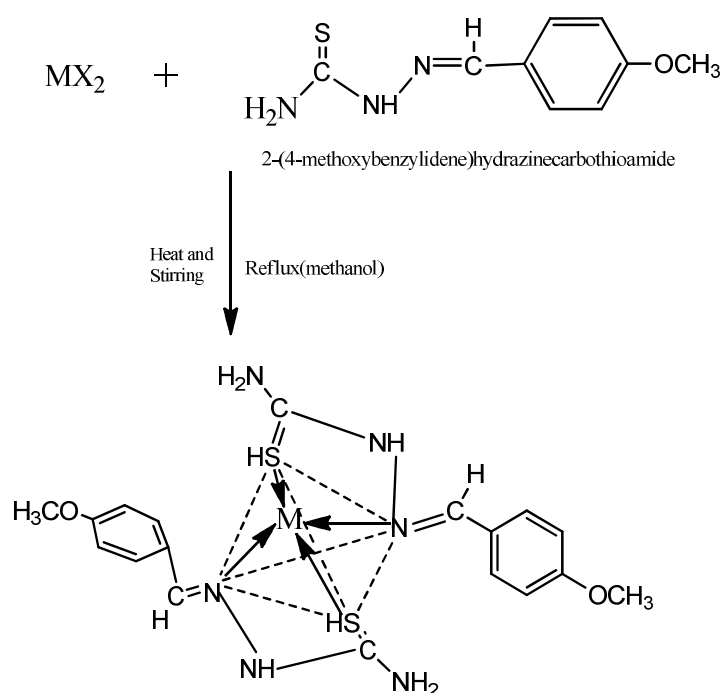
3.3 Characterizations by Magnetic Susceptibility

3.3.1 Measurement of magnetic susceptibility

The measurements of magnetic susceptibilities were made at about constant temperature; Curie-law was used and was calculated from the equation.

$$\mu_{\text{eff}} = 2.83 \sqrt{\chi_m^{\text{corr}} \cdot T} \text{ B.M.} \quad (2)$$

Thus μ_{eff} obtained is known as the effective magnetic moment. All the values and weight were expressed in C.G.S. units. The observed values of the effective magnetic moment (μ_{eff}) of the complexes at room temperature are given in Table 2. From the above data, it is showed that



Scheme 6. Synthetic pathway of Schiff base Ligand (L^4) Metal complex where, $M=\text{Cd(II)}$ ions

Table 1. Physical characteristics and analytical data of ligands and complexes

| Compound/empirical formula | Formula weight | Color | Yield (%) | Melting point/decomposition temp.(°C) |
|---|----------------|-----------------|-----------|---------------------------------------|
| Ligand (L ¹) C ₈ H ₉ ON ₃ S | 195 | off white | 80 % | 215°C - 217°C |
| [Zn (L ¹) ₂].2H ₂ O | 491.38 | cream color | 67 % | above 300°C |
| [ZnC ₁₆ H ₁₆ O ₂ N ₆ S ₂].2H ₂ O | | | | |
| [Ni (L ¹) ₂].H ₂ O | 466.93 | yellow green | 70 % | 275°C - 280°C |
| [NiC ₁₆ H ₁₆ O ₂ N ₆ S ₂].H ₂ O | | | | |
| [Mn (L ¹) ₂].H ₂ O | 462.94 | golden rod | 65 % | 275°C - 280°C |
| [MnC ₁₆ H ₁₆ O ₂ N ₆ S ₂].H ₂ O | | | | |
| [Sn (L ¹) ₂] | 508.71 | greenish yellow | 60% | 240°C - 250°C |
| [SnC ₁₆ H ₁₆ O ₂ N ₆ S ₂] | | | | |
| Ligand (L ²) C ₁₄ H ₁₁ O ₃ N | 241 | yellow | 65 % | 241°C - 245°C |
| [Co(L ²) ₂].2H ₂ O | 576.93 | golden rod | 56 % | above 300°C |
| [CoC ₂₈ H ₁₈ O ₆ N ₂].2H ₂ O | | | | |
| Ligand (L ³) C ₉ H ₁₁ N ₃ OS | 209 | off white | 62% | 145°C - 150°C |
| [Cd(L ³) ₂] | 530.41 | white | 75 % | 260°C - 265°C |
| [CdC ₁₈ H ₂₂ O ₂ N ₆ S ₂] | | | | |

Table-2. Data for the determination of molar conductivity

| Name of complex | Observed conductivity (ohm ⁻¹ cm ² mol ⁻¹) | Molar conductance $\Lambda = (1000/c) \times \text{specific conductance } S\text{cm}^2\text{mol}^{-1}$ | μ_{eff} in B.M. | No. of unpaired electron |
|---|--|--|----------------------------|--------------------------|
| [Zn (L ¹) ₂].2H ₂ O | 3 | 3 | 0.567 | — |
| [ZnC ₁₆ H ₁₆ O ₂ N ₆ S ₂].2H ₂ O | | | | |
| [Ni (L ¹) ₂].H ₂ O | 6 | 6 | 1.471 | — |
| [NiC ₁₆ H ₁₆ O ₂ N ₆ S ₂].H ₂ O | | | | |
| [Mn (L ¹) ₂].H ₂ O | 8 | 8 | 2.576 | 1 |
| [MnC ₁₆ H ₁₆ O ₂ N ₆ S ₂].H ₂ O | | | | |
| [Sn (L ¹) ₂] | 9 | 9 | 0.639 | — |
| [SnC ₁₆ H ₁₆ O ₂ N ₆ S ₂] | | | | |
| [Co(L ²) ₂].2H ₂ O | 8 | 8 | 4.017 | 3 |
| [CoC ₂₈ H ₁₈ O ₆ N ₂].2H ₂ O | | | | |
| [Cd(L ³) ₂] | 6 | 6 | 0.461 | — |
| [CdC ₁₈ H ₂₂ O ₂ N ₆ S ₂] | | | | |

the Zn(II), Ni(II), Sn(II) and Cd(II) ions complexes are diamagnetic and Mn(II) and Co(II) ions complexes are paramagnetic in nature [12-13].

3.4 Measurement of IR Spectra

At first the complexes heat six hours and KBr overnight in the oven. Then the complexes and KBr grind with a pestle in a mortar. Infrared spectra disc were recorded as KBr with a NICOLET 310, FTIR spectrophotometer, Belgium, from 4000-225 cm⁻¹.

3.4.1 IR spectra of schiff base ligand C₈H₉ON₃S (L¹) and its metal complexes

The spectrum of ligand showed a strong absorption band at 1616 cm⁻¹ due to the azomethine $\nu(\text{C}=\text{N})$ stretching frequency of the free ligand [14-18] indicating that the condensation has taken place between the CHO moiety of salicylaldehyde and -NH₂ moiety of thiosemicarbazide. The IR spectra of the free ligand (Fig. 1) showed two bands at 3320 cm⁻¹ and 3174 cm⁻¹ may be attributed to the free -NH₂ and $\nu(\text{N}-\text{H})$ groups respectively. These bands

remain in the same region in all complexes spectra, suggesting nonparticipation in the coordination of one terminal $-NH_2$ group in thiosemicarbazone [15,19-21]. The band observed at 3444 cm^{-1} was assigned to the $\nu(O-H)$ of hydroxyl group [14,15,22]. The strong band 776 cm^{-1} for $\nu(C=S)$ indicated that C=S bond was present in the Schiff base ligand [14,22].

In order to determine the mode of coordination of ligand to metal in complexes, IR spectrum of the ligand was compared with IR spectrum of metal complexes (Fig. 2). The band at 1616 cm^{-1} due to the azomethine $\nu(C=N)$ stretching frequency of the free ligand that shifted to a lower frequency in the spectra of the Zn (II) complex at 1607 cm^{-1} which indicated the coordination

through azomethine N atom. The band 3444 cm^{-1} due to the $\nu(O-H)$ of the hydroxyl group in the IR spectra of the ligand was absent and shifted to lower absorption frequency in the IR spectra of Ni(II) complex indicated the coordination through the phenolic oxygen [23,24]. This is confirmed by the shift of $\nu(C-O)$ stretching vibration observed at 1266 cm^{-1} in the spectra of free ligand to 1285 cm^{-1} stretching vibration of complex after coordination [16], which corresponds to forming of weaker C-O(Zn) bond comparing to C-O(H) and confirms coordination of ligand to Ni(II) via deprotonated phenolic oxygen [25,26]. Also the medium intensity bands observed at 566 cm^{-1} is attributed to M-O and 448 cm^{-1} is attributed to M-N bonds [27]. IR spectral components of the synthesized complexes are shown in Table 3.

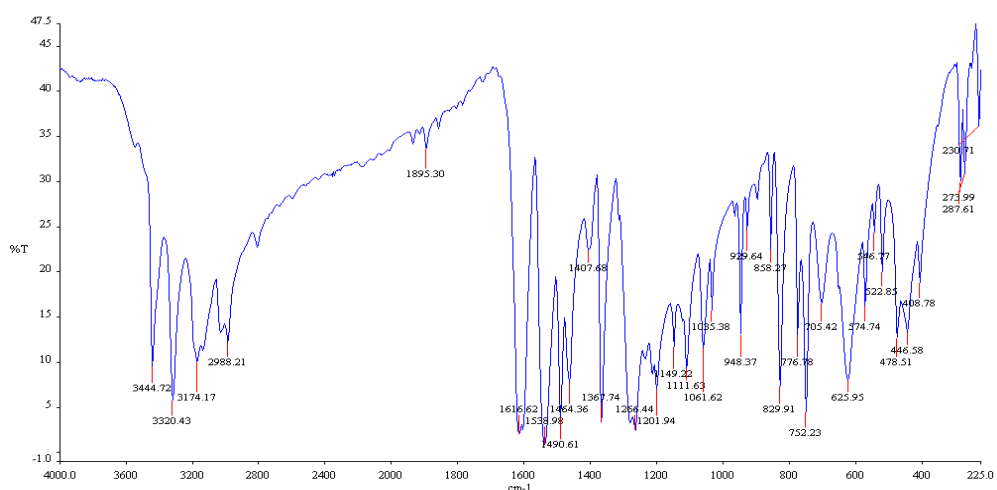


Fig. 1. IR spectra of Schiff base LIGAND $C_8H_9ON_3S$ (L^1)

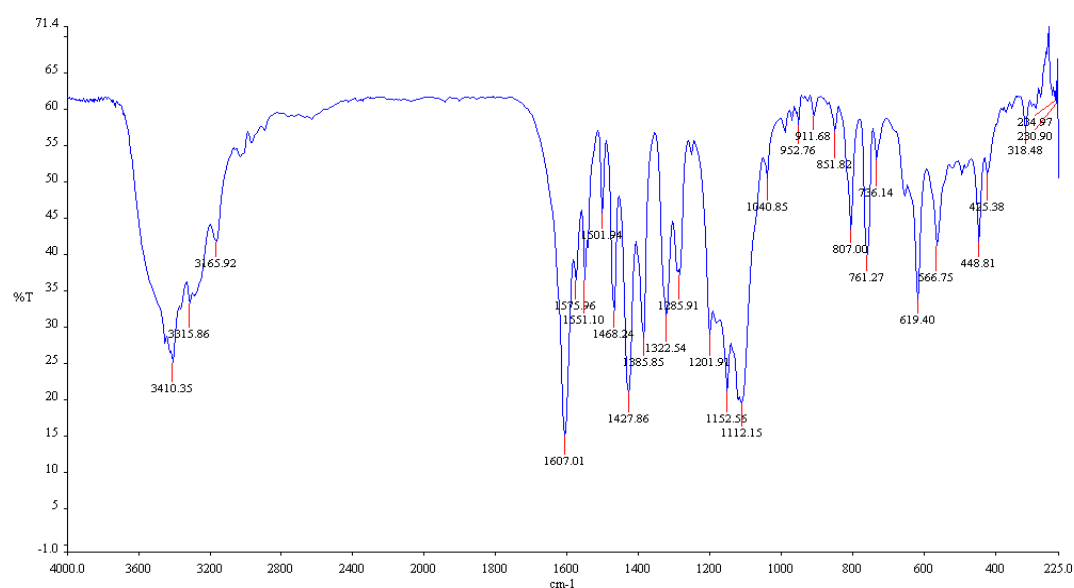


Fig. 2. IR spectra of $[ZnC_{16}H_{16}O_2N_6S_2].2H_2O$ complex

Table 3. FTIR spectral data of the LIGAND C₈H₉ON₃S (L¹) and it's metal complexes (in cm⁻¹)

| Ligand / metal complexes | IR/cm ⁻¹ | | | | |
|---|---------------------|-------------------|-------------------|-------------------|-------------------|
| | $\nu(\text{O-H})$ | $\nu(\text{C=N})$ | $\nu(\text{C-O})$ | $\nu(\text{M-O})$ | $\nu(\text{M-N})$ |
| C ₈ H ₉ ON ₃ S | 3444 | 1616 | 1266 | - | - |
| [ZnC ₁₆ H ₁₆ O ₂ N ₆ S ₂].2H ₂ O | 3410 | 1607 | 1285 | 566 | 448 |
| [NiC ₁₆ H ₁₆ O ₂ N ₆ S ₂].H ₂ O | 3412 | 1607 | 1294 | 567 | 457 |
| [MnC ₁₆ H ₁₆ O ₂ N ₆ S ₂].H ₂ O | 3413 | 1600 | 1296 | 570 | 442 |
| [SnC ₁₆ H ₁₆ O ₂ N ₆ S ₂] | 3436 | 1610 | 1286 | 594 | 458 |

3.4.2 IR spectra of schiff base ligand C₁₄H₁₁O₃N (L²) and it's metal complex

The bands at 1735 cm⁻¹ and 3420 cm⁻¹ due to carbonyl (C=O) and NH₂ stretching vibrations of the starting reagents respectively were absent in the spectra of ligand and a strong new band at 1620 cm⁻¹ appeared which assigned to the azomethine (HC=N) linkage, a fundamental feature of Schiff base ligand [28,29]. This indicated that amino and aldehyde moieties of the starting reagents have been converted into the azomethine moiety. The bands at 1320 cm⁻¹ due to $\nu(\text{C-O})$ of the phenolic group and 3410 cm⁻¹ due to the phenolic $\nu(\text{OH})$ were also observed in the spectra of ligand [23]. The bands at 1680 cm⁻¹ due to $\nu(\text{C=O})$ stretching vibration and 3080 cm⁻¹ due to carboxylic – $\nu(\text{OH})$ were observed in the IR spectra of ligand [30-33].

The band at 1620 cm⁻¹ due to the azomethine – HC=N stretching vibration was shifted to a lower frequency at 1541 cm⁻¹ in the metal complex compared to free ligand, suggested the coordination of metal ion through nitrogen of azomethine group [34-36]. The N atom of azomethine would reduce the electron density in the azomethine link and thus lower the –HC=N absorption after coordination. This is further substantiated by the presence of a new band at 457 cm⁻¹ assignable to $\nu(\text{M-N})$. The disappearance of phenolic $\nu(\text{OH})$ band at 3410 cm⁻¹ in Co(II) complex suggested the coordination by the phenolic oxygen after deprotonation to the metal ions. This is further supported by shifting of $\nu(\text{C-O})$ phenolic band at 1320 cm⁻¹ to lower wave number at 1305 cm⁻¹ in the metal complex. The appearance of a new band at 590cm⁻¹ due to $\nu(\text{M-O})$ in the Co(II) complex which further substantiates. The band at 1680 cm⁻¹ assigned to $\nu(\text{C=O})$ in the spectra of ligand also shifted to the lower frequency range in the metal complex. That suggested the involvement of oxygen atom of carboxylic $\nu(\text{OH})$ group to the coordination with metal ions. The comparison of the IR spectra of the Schiff base and it's metal chelates indicated that the Schiff

base ligand coordinated to metal ions by three donor atoms representing the ligand acting in a tri-dentative manner. Spectral data of [CoC₂₈H₁₈O₆N₂].2H₂O is shown in Table 4.

In order to determine the mode of coordination of ligand to metal in complexes IR spectrum of the ligand was compared with IR spectrum of metal complexes [14,23]. The band at 1616 cm⁻¹ due to the azomethine $\nu(\text{C=N})$ stretching frequency of the free ligand that shifted to a lower frequency in the spectra of the Ni(II) complex (figure-13) at 1607cm⁻¹ indicating the coordination through N atom [5-9]. The band 3444 cm⁻¹ due to the $\nu(\text{O-H})$ of the hydroxyl group in the IR spectra of the ligand was absent and shifted to lower absorption frequency in the IR spectra of Ni(II) complex indicated the coordination through the phenolic oxygen [22,24]. This is confirmed by the shift of $\nu(\text{C-O})$ stretching vibration observed at 1266 cm⁻¹ in the spectra of free ligand to 1294 cm⁻¹ stretching vibration of complex after coordination [16], which corresponds to forming of weaker C-O(Ni) bond comparing to C-O(H) and confirms coordination of ligand to Ni(II) via deprotonated phenolic oxygen. Also, the medium intensity bands observed at 567 cm⁻¹ is attributed to M-O and 457cm⁻¹ is attributed to M-N bonds [27].

The band at 1616 cm⁻¹ due to the azomethine $\nu(\text{C=N})$ stretching frequency of the free ligand that shifted to a lower frequency in the spectra of the Mn(II) complex at 1600 cm⁻¹ indicating the coordination through N atom. The band 3444 cm⁻¹ due to the $\nu(\text{O-H})$ of the hydroxyl group in the IR spectra of the ligand was absent and shifted to lower absorption frequency in the IR spectra of Mn(II) complex indicated the coordination through the phenolic oxygen. This is confirmed by the shift of $\nu(\text{C-O})$ stretching vibration observed at 1266 cm⁻¹ in the spectra of free ligand to 1296 cm⁻¹ stretching vibration of complex after coordination, which corresponds to forming of weaker C-O(Mn) bond comparing to C-O(H) and confirms coordination of ligand to Mn(II) via deprotonated phenolic oxygen [5,17].

Also, the medium intensity bands observed at 570cm^{-1} is attributed to M-O and 442cm^{-1} is attributed to M-N bonds [27].

The band at 1616cm^{-1} due to the azomethine $\nu(\text{C}=\text{N})$ stretching frequency of the free ligand that shifted to a lower frequency in the spectra of the Sn(II) complex at 1610cm^{-1} indicating the coordination through N atom. The band 3444cm^{-1} due to the $\nu(\text{O-H})$ of the hydroxyl group in the IR spectra of the ligand was absent and shifted to lower absorption frequency in the IR spectra of Sn(II) complex indicated the coordination through the phenolic oxygen. This is confirmed by the shift of $\nu(\text{C-O})$ stretching vibration observed at 1266cm^{-1} in the spectra of free ligand to 1286cm^{-1} stretching vibration of complex after coordination, which corresponds to forming of weaker C-O(Sn) bond comparing to C-O(H) and confirms coordination of ligand to Sn(II) via deprotonated phenolic oxygen. Also, the medium intensity bands observed at 594cm^{-1} is attributed to M-O and 458cm^{-1} is attributed to M-N bonds.

3.4.3 IR spectra of schiff base ligand $\text{C}_9\text{H}_{11}\text{N}_3\text{O}_3$ (L^3) and its metal complex

The peaks obtained at 3406cm^{-1} and 3291cm^{-1} may be assigned to symmetric and asymmetric $\nu(\text{N-H})$ stretching frequency of primary amino group. The broad peak obtained between 3282 and 2829cm^{-1} may be assigned to overlapping of peaks of hydrogen-bonded $\nu(\text{N-H})$ and aromatic C-H stretching frequency. The bands obtained between 1183cm^{-1} and 1252cm^{-1} in ligand were due to $\nu(\text{-OCH}_3)$ groups (Table-5). The peaks observed at 1606cm^{-1} and 834cm^{-1} may be assigned to $\nu(\text{C}=\text{N})$ and $\nu(\text{C}=\text{S})$ [37-39].

The bands at 1606cm^{-1} and 834cm^{-1} assigned to $\nu(\text{C}=\text{N})$ and $\nu(\text{C}=\text{S})$ modes and these bands shifted towards lower frequency in the spectra of Cd(II) complex (Table-5), which indicated that coordination takes place through nitrogen of $\nu(\text{C}=\text{N})$ group and sulphur of $\nu(\text{C}=\text{S})$ group. At lower frequency, the complex exhibited new bands at 540 and 397cm^{-1} which further supported the coordination site $\nu(\text{M-N})$ and $\nu(\text{M-S})$ vibrations.

3.5 Characterization by UV-visible Spectra

The electronic spectral data for the ligand and their metal complex recorded in DMSO are summarized in Table-6. There are two absorption bands, assigned to $n-\pi^*$ and $\pi-\pi^*$ transitions, in the electronic spectrum of the ligand. These transitions are also found in the spectra of the complexes, but they are shifted towards lower and higher frequencies, indicating the coordination of the ligand to the metallic ions [40]. The UV spectra of the ligand show three absorption bands at 260nm , 310nm and 355nm . The first two bands are assigned to $\pi-\pi^*$ transitions of azomethine chromospheres and a benzene ring and the third is assigned to $n-\pi^*$ transition of a lone pair of electrons of an azomethine nitrogen and an antibonding π orbital. The absorption band $n-\pi^*$ at 355nm due to an imine group in the ligand, whereas for the zinc complex, the same was observed at 390nm with weak absorption intensity which indicates the coordination of zinc with imine group [41]. The zinc complex shows only the charge transfer transition which can be assigned to charge transfer from the ligand to the metal and vice versa, no d-d transitions are expected for d^{10} Zn(II) complex [42].

Table 4. FTIR spectral data of the ligand L^2 and $[\text{CoC}_{28}\text{H}_{18}\text{O}_6\text{N}_2].2\text{H}_2\text{O}$ (in cm^{-1})

| Ligand / metal complexes | IR/ cm^{-1} | | | | | |
|--|----------------------|--------------------------|--------------------------|-------------------|-------------------|-------------------|
| | $\nu(\text{O-H})$ | $\nu(\text{C}=\text{N})$ | $\nu(\text{C}=\text{O})$ | $\nu(\text{C-O})$ | $\nu(\text{M-O})$ | $\nu(\text{M-N})$ |
| $\text{C}_{14}\text{H}_{11}\text{O}_3\text{N}$ | 3410 | 1620 | 1680 | 1320 | - | - |
| $[\text{CoC}_{28}\text{H}_{18}\text{O}_6\text{N}_2].2\text{H}_2\text{O}$ | 3436 | 1541 | 1598 | 1305 | 590 | 457 |

Table 5. FTIR spectral data of the ligand L^3 and its Cd(II) metal complex (in cm^{-1})

| Ligand / metal complexes | IR/ cm^{-1} | | | |
|--|--------------------------|--------------------------|-------------------|-------------------|
| | $\nu(\text{C}=\text{N})$ | $\nu(\text{C}=\text{S})$ | $\nu(\text{M-N})$ | $\nu(\text{M-S})$ |
| Ligand (L^3) | 1606 | 834 | - | - |
| $\text{C}_9\text{H}_{11}\text{N}_3\text{O}_3$ $[\text{Cd}(\text{L}^3)_2]$ $[\text{CdC}_{18}\text{H}_{22}\text{O}_2\text{N}_6\text{S}_2]$ | 1574 | 821 | 528 | 397 |

The UV-Vis absorption spectra of the ligand and complex were recorded after dissolving into DMSO solvent at room temperature. There are two absorption bands, assigned to $n-\pi^*$ and $\pi-\pi^*$ transitions, in the electronic spectrum of the ligand. These transitions are also found in the spectra of the complexes, but they are shifted towards lower and higher frequencies, confirming the coordination of the ligand to the metallic ions [43]. The electronic spectrum of ligand exhibits three intense absorption peaks at 260 nm, 310 nm and 350nm. The first and second peaks were attributed to benzene $\pi-\pi^*$ and imino $\pi-\pi^*$ transitions and the third peak in the spectra was assigned to $n-\pi^*$ transition [44]. The electronic spectra of the Ni(II) complex with an electronic configuration of d^8 shows three new absorption bands in the visible region and these three bands of the transitions $^1A_{1g} \rightarrow ^1A_{2g}$ (355nm), $^1A_{1g} \rightarrow ^1B_{1g}$ (380 nm) and $^1A_{1g} \rightarrow ^1E_g$ (420 nm) were observed in the spectra of a square-planar Ni(II) complex [45,46].

The UV-Vis absorption spectra of the ligand and complex were recorded after dissolving into DMSO solvent at room temperature. There are two absorption bands, assigned to $n-\pi^*$ and $\pi-\pi^*$ transitions, in the electronic spectrum of the ligand. These transitions are also found in the spectra of the complexes, but the ligand to the metallic ions [47]. The electronic spectrum of ligand exhibits three intense absorption peaks at 260 nm, 310 nm and 350nm. The first and second peaks were attributed to benzene $\pi-\pi^*$ and imino $\pi-\pi^*$ transitions and the third peak in the spectra was assigned to $n-\pi^*$ transition. Due to Forbidden transition, several bands were observed in the visible region of Mn(II) complex, and the band at 430 nm is attributed to (d-d) transition of type $^6A_1 \rightarrow ^4T_2$.

The electronic absorption spectra of ligand L^1 and its Sn (II) complex in DMSO solution were carried out in the range of 200-800 nm at room temperature. There is a shift of the bands to longer wavelength in spectra of the complex is a good evidence of complex formation. There were various bands in the ligand spectra assigned to inter ligand and charge transfer of $n-\pi^*$ transitions according to their energies and intensities. Ligand exhibits three intense absorption peaks at 260 nm, 310 nm and 350 nm. The first and second peaks were attributed to benzene $\pi-\pi^*$ and imino $\pi-\pi^*$ transitions and the third band in the spectra was assigned to $n-\pi^*$ transition. The complex showed an intense band at 410nm due to the $n-\pi^*$ transition of azomethine chromosphere and the band at 340 nm may be assigned as charge transfer band. It has been reported that the metal is capable of forming $dn-p\pi^*$ bonds with ligands containing nitrogen as the donor atom. The Sn atom has its 5d orbital completely vacant and hence $Sn \leftarrow N$ bonding can take place by the acceptance of the lone pair of electrons from the azomethine nitrogen of the ligand [48-50].

The magnetic moment and electronic spectra are very effective in the evaluation of results obtained by other methods of structural investigation. Information regarding the geometry of the complex of Co(II) ions was obtained from electronic spectral studies and magnetic moments (Table 7). The electronic spectra of ligand and their metal complexes were recorded in DMSO. Electronic spectrum of ligand shows strong absorption band at 330 nm region can be assigned to the $n \rightarrow \pi^*$ transition of the azomethine group of ligand, which slightly shifted to a lower frequency in the spectra of the complex, indicating that the azomethine nitrogen atom is

Table 6. Magnetic moments and electronic spectral data for ligand (L^1) and its metal complexes

| Compound | λ_{max} n.m | Wave number cm^{-1} | μ_{eff} B.M | Assignment |
|-----------------------------------|---------------------|-----------------------|-----------------|---------------------------------|
| $C_8H_9ON_3S$ | 260 | 38461 | — | $\pi \rightarrow \pi^*$ |
| | 310 | 32258 | | $\pi \rightarrow \pi^*$ |
| | 350 | 38571 | | $n \rightarrow \pi^*$ |
| $[NiC_{16}H_{16}O_2N_6S_2].H_2O$ | 355 | 28169 | 1.469 | $^1A_{1g} \rightarrow ^1A_{2g}$ |
| | 380 | 26315 | | $^1A_{1g} \rightarrow ^1B_{1g}$ |
| | 420 | 23809 | | $^1A_{1g} \rightarrow ^1E_g$ |
| $[ZnC_{16}H_{16}O_2N_6S_2].2H_2O$ | 265 | 37735 | 0.5197 | C.T (M \rightarrow L) |
| | 320 | 31250 | | C.T (M \rightarrow L) |
| | 390 | 25641 | | C.T (M \rightarrow L) |
| $[MnC_{16}H_{16}O_2N_6S_2].H_2O$ | 325 | 30769 | 2.507 | $^6A_1 \rightarrow ^4T_2$ |
| | 380 | 26315 | | |
| | 430 | 23255 | | |

Table 7. The electronic spectral data and magnetic moments for ligand (L²) and its metal complex

| Compound | λ_{max} n.m | Wave number cm^{-1} | μ_{eff} B.M | Assignment |
|--|---------------------|-----------------------|-----------------|--|
| C ₁₄ H ₁₁ O ₃ N | 330 | 30303 | - | n→π* |
| [CoC ₂₈ H ₁₈ O ₆ N ₂].2H ₂ O | 264 | 37878 | 4.0137 | Charge transfer(C.T) |
| | 274 | 36496 | | C.T (M→L) |
| | 400 | 25000 | | ⁴ T _{1g} (F)→ ⁴ T _{1g} (P) |

involved in coordination to the metal ion. The Co(II) complex was found the magnetic moment 4.0137 B.M which indicated the three unpaired electrons per Co(II) ion attaining an octahedral environment. The electronic spectrum of Co(II) complex shows bands at 264nm and 274nm are assignable to metal-ligand charge transfer band and the band 400nm is assignable to ⁴T_{1g}(F)→⁴T_{1g}(P) transition.

The electronic spectral data for the ligand and its metal complex recorded in DMSO are summarized in Table-8. There are two absorption bands, assigned to n→π* and π→π* transitions, in the electronic spectrum of the ligand. These transitions are also found in the spectra of the complexes, but they are shifted towards lower and higher frequencies, indicating the coordination of the ligand to the metallic ions. The UV spectra of the ligand show three absorption bands at 280 nm, 330 nm and 350 nm. The first two bands are assigned to π→π* transitions of azomethine chromospheres and a benzene ring and the third is assigned to n→π* transition of a lone pair of electrons of an azomethine nitrogen and an anti-bonding π orbital. The absorption band n→π* at 350nm due to an imine group in the ligand, whereas for the Cd(II) complex, the same was observed at 400 nm with weak absorption intensity which indicates the coordination of cadmium with imine group. The cadmium complex shows only the charge transfer transition which can be assigned to charge transfer from the ligand to the metal and vice versa, no d-d transition are expected for diamagnetic d¹⁰ Cd(II) complex. The shifting of ligand absorption in the UV region, in the spectra of the complex confirming the coordination of the ligand to metal like Cd (II) ions.

3.6 Thermogravimetric Analysis

3.6.1 Zn(II), Ni(II), Mn(II) and Sn(II) complexes of ligand C₈H₉ON₃S (L¹)

The thermal decomposition analysis of solid Zn(II), Ni(II), Mn(II) and Sn(II) metal complexes were carried out under nitrogen atmosphere and heating rate was suitably controlled at 30°C min⁻¹ and the weight loss was measured from the ambient temperature up to 800°C. The data from TGA and DTG clearly indicated that the decomposition of the complexes proceeds in three or four steps. There were some minor steps and asymmetry of TGA/DTG curves also observed. The weight losses for each complex were calculated within the corresponding temperature ranges. The different thermodynamic parameters are listed in Table-9 and the decomposition curves are shown as supplementary materials.

The TGA and DTG curve of Zn(II) complex indicated that the complex was decomposed into four main steps. In the first step of decomposition, two molecules of water were lost at the temperature range of 85-110°C (calculated 7.36%, experimental 7.20%). In this temperature range, the loss of water molecules indicates that the water molecules are of lattice type [51,52]. In the temperature range 130-335°C (calculated 24.00% and experimental 23.10%), the part of ligand-2CSNH₂ was decomposed at the second step. The other part of the ligand 2C₆H₄O- were decomposed in the third step at 335-740°C (calculated 37.50%, experimental 32.00%). At above 750°C temperature the complex was decomposed and removed as Zn/ZnO

Table-8. Magnetic moments and electronic spectral data for ligand (L³) and its Cd(II) complex

| Compound | λ_{max} n.m | Wave number cm^{-1} | μ_{eff} B.M | Assignment |
|---|---------------------|-----------------------|-----------------|------------|
| C ₉ H ₁₁ N ₃ OS | 280 | 35714 | - | π→π* |
| | 330 | 30303 | | π→π* |
| | 350 | 28571 | | n→π* |
| [CdC ₁₈ H ₂₂ O ₂ N ₆ S ₂] | 295 | 33898 | 0.4606 | C.T (M→L) |
| | 340 | 29412 | | C.T (M→L) |
| | 400 | 25000 | | C.T (M→L) |

(calculated 31.14%, experimental 37.70%) polluted with few carbon atoms [53].

The TGA and DTG curve of Ni(II) complex confirmed that the complex was decomposed into four main steps. The 1st step involves the removal of one molecule of hydrated water (calculated 3.87%, experimental 4.00% weight) at temperature range 80-190°C [54,55]. In the 2nd step the part of the ligand $2C_6H_4O^-$ was decomposed at 280-350°C (calculated 39.59%, experimental 34.82% weight). At the 3rd step the fragmentation of coordinated ligand $2C_2H_4N_3S$ was decomposed from the complex at the temperature range 360-750°C (calculated 43.90%, experimental 44.20% weight) and above 750°C temperature the complex was completely decomposed and removed as Ni/NiO (calculated 12.64%, experimental 16.98%).

In the case of Mn(II) complex, the TGA and DTG curve indicated that the complex was decomposed into four main steps. At 1st step, one molecule of hydrated water was removed at 80-180°C (calculated 3.90%, experimental 4.00%) [54,55]. Then the dehydrated complex was gradually decomposed and the part of ligand $2C_6H_4O^-$ was removed at the temperature range

180-350°C (calculated 39.92%, experimental 38.10%). The 3rd step involves the decomposition of the ligand part $2CH_3N_2S$ at the temperature range 350-770°C (calculated 32.54%, experimental 32.22%). At above 770°C temperature finally the complex was completely decomposed and removed as Mn/MnO (calculated 23.64%, experimental 25.68%).

The Sn(II) complex showed high thermal stability and decomposed above 170°C, indicating the absence of any lattice water molecules. This complex was decomposed into four main steps. At first step, the part of ligand ($-2CH_2NS$) was decomposed at temperature 170-275°C (calculated 23.67%, experimental 22.00%). In 2nd step, the decomposition of ($-2CHN-$) moiety was taken place at temperature 275-330°C (calculated 12.0%, experimental 10.65%). The ligand part ($2C_6H_4O^-$) were decomposed at the 3rd step at temperature range 330-750°C (calculated 36.29%, experimental 36.10%) and finally, the complex was completely decomposed and removed as Sn/SnO (calculated 28.04%, experimental 31.25%).

Table- 9. Thermal data of Zn(II), Ni(II), Mn(II), Sn(II), Cd(II) and Co(II) complexes

| Complexes | Steps | Temperature range/ °C | DTG Peak/ °C | TG mass loss% calc./found | Assignments |
|---|-----------------|-----------------------|--------------|---------------------------|---|
| [ZnC ₁₆ H ₁₆ O ₂ N ₆ S ₂].2H ₂ O | 1 st | 85-110 | 97 | 7.36/7.20 | 2H ₂ O |
| | 2 nd | 130-335 | 278 | 24.00/23.10 | 2CSNH ₂ |
| | 3 rd | 335-740 | 350 | 37.50/32.00 | 2C ₆ H ₄ O ⁻ |
| | 4 th | >750 | | 31.14/37.7 | Zn/ZnO |
| [NiC ₁₆ H ₁₆ O ₂ N ₆ S ₂].H ₂ O | 1 st | 80-190 | 180 | 3.87/4.00 | H ₂ O |
| | 2 nd | 280-350 | 295 | 39.59/34.82 | 2C ₆ H ₄ O ⁻ |
| | 3 rd | 360-750 | 382 | 43.90/44.20 | 2C ₂ H ₄ N ₃ S |
| | 4 th | >750 | | 12.64/16.98 | Ni/NiO |
| [MnC ₁₆ H ₁₆ O ₂ N ₆ S ₂].H ₂ O | 1 st | 80-180 | 118 | 3.90/4.00 | H ₂ O |
| | 2 nd | 180-350 | 290 | 39.92/38.10 | 2C ₆ H ₄ O ⁻ |
| | 3 rd | 350-770 | | 32.54/32.22 | 2CH ₃ N ₂ S |
| | 4 th | >770 | | 23.64/25.68 | Mn/MnO |
| [SnC ₁₆ H ₁₆ O ₂ N ₆ S ₂] | 1 st | 170-275 | 240 | 23.67/22.00 | 2CH ₂ NS |
| | 2 nd | 275-330 | 290 | 12.00/10.65 | 2CHN- |
| | 3 rd | 330-750 | 370 | 36.29/36.10 | 2C ₆ H ₄ O ⁻ |
| | 4 th | >750 | | 28.04/31.25 | Sn/SnO |
| [CoC ₂₈ H ₁₈ O ₆ N ₂].2H ₂ O | 1 st | 40-110 | 65 | 6.28/6.32 | 2H ₂ O |
| | 2 nd | 110-480 | 400 | 51.31/49.20 | 2C ₈ H ₅ O ₂ N |
| | 3 rd | 480-650 | 548 | 32.12/28.80 | 2C ₆ H ₄ O ⁻ |
| | 4 th | >650 | | 10.29/15.72 | Co/CoO |
| [CdC ₁₈ H ₂₂ O ₂ N ₆ S ₂] | 1 st | 230-455 | 282 | 50.53/49.23 | 2C ₈ H ₈ ON |
| | 2 nd | 455-740 | 570 | 28.28/27.05 | 2CH ₃ N ₂ S |
| | 3 rd | >740 | | 21.19/24.00 | Cd/CdO |

3.6.2 Co (II) complex of ligand $C_{14}H_{11}O_3N$ (L^2)

TGA was carried out for solid Co(II) metal complex under N_2 flow. The heating rate was suitably controlled at $30^\circ C \text{ min}^{-1}$ and the weight loss was measured from the ambient temperature up to $800^\circ C$. The thermogram of complex exhibits three clear-cut decomposition stages in (Fig. 3). The first stage with estimated mass loss of 6.32% (calculated mass loss 6.28%) within the temperature range $40\text{--}110^\circ C$ corresponding to the loss of water molecules [56,57]. The second stage occurs at $110\text{--}480^\circ C$, with a mass loss of 49.20% (calculated 51.31%), corresponding to the loss of $2C_8H_5O_2N$ parts of the ligand. The third stage of decomposition occurs at the temperature range $480\text{--}650^\circ C$, with a mass loss of 28.80% (calculated 32.12%), corresponding to the loss of $2C_6H_4O$ moiety. At above $650^\circ C$ temperature, the complex was completely decomposed and removed as of 15.72% (calculated 10.29%). The different TG and DTG data are given in Table 9.

3.6.3 Cd(II) complex of ligand $C_9H_{11}N_3OS$ (L^3)

Thermogravimetric analysis of solid Cd(II) metal complex under N_2 flow. The heating rate was suitably controlled at $30^\circ C \text{ min}^{-1}$ and the weight loss was measured from the ambient temperature up to $800^\circ C$. The TGA curve of the Cd(II) complex showed no mass loss up to $230^\circ C$, indicating the absence of lattice / coordinated water [58,59] and the high thermal

stability of the complex. The thermogram of Cd(II) complex is given in Fig. 4. 24, which shows two stage decomposition pattern. The first stage was exhibited a maximum mass loss of 49.23% (calculated 50.53%) of ligand part ($2C_8H_8ON$) at $230\text{--}455^\circ C$. The second stage occurs at $455\text{--}740^\circ C$, with a mass loss of 27.05% (calculated 28.28%) attributed to the loss of $(2CH_3N_2S)$ moiety. Finally at above $750^\circ C$ temperature the complex was completely decomposed and removed as Cd/CdO of 24.0% (calculated 21.19%). The different TG and DTG data are given in Table 9.

3.6.4 Antibacterial activity

The prime objective of performing the antibacterial screening is to determine the susceptibility of the pathogenic microorganism to test the compound which, in turn, is used to a selection of the compound as a therapeutic agent. The free Schiff base ligand and their metal complexes were screened for their antibacterial activity against strains the *Bacillus cereus* ATCC25923, *Streptococcus agalactiae*, *Escherichia coli* ATCC 25922, *Shigella dysenteriae*. The compounds were tested at a concentration of $30 \mu\text{g}/0.01 \text{ mL}$ in DMSO solution using the paper disc diffusion method with Kanamycin as standard. The susceptibility zones were measured in diameter (mm) and the result are listed in Table 10. The susceptibility zones were the clear zones around the discs killing the bacteria.

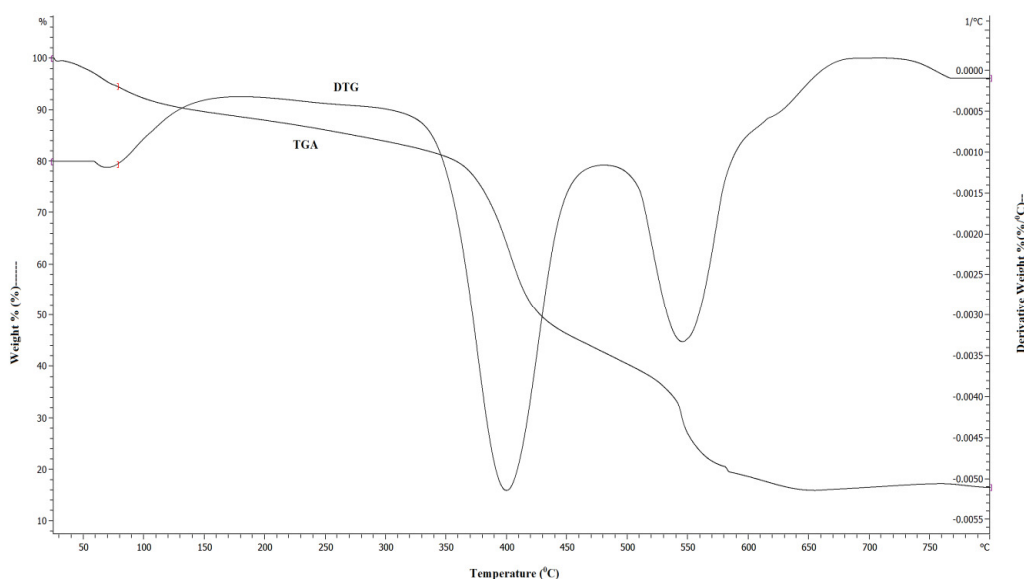


Fig. 3. TGA and DTG curve of $[CoC_{28}H_{18}O_6N_2] \cdot 2H_2O$

Table 10. Antibacterial activities of the complexes

| Bacterials strains | Zone of inhibition, diameter in mm | | | | | | |
|-------------------------------------|------------------------------------|-----------------------|-----------------------|-----------------------|-----------------------|-----------------------|-----------------------|
| | A (10 µg /disc) | B (10 µg /disc) | C (10 µg /disc) | D (10 µg /disc) | E (10 µg /disc) | F (10 µg /disc) | K (30 µg /disc) |
| Gram positive | | | | | | | |
| <i>Bacillus cereus</i> | 22 | 10 | 19 | 12 | 11 | 14 | 36 |
| <i>Streptococcus agelactiae</i> | 19 | 09 | 21 | 08 | 14 | 16 | 35 |
| Gram negative | | | | | | | |
| <i>Escherichia coli</i> | 23 | 12 | 24 | 09 | 12 | 18 | 32 |
| <i>Shigella dysenteriae</i> | 09 | 11 | 10 | 12 | 08 | 14 | 36 |

Where, A = $[C_{16}H_{16}ZnO_2N_6S_2].2H_2O$, B = $[C_{16}H_{16}NiO_2N_6S_2].H_2O$, C = $[C_{16}H_{16}MnO_2N_6S_2].H_2O$, D = $[C_{16}H_{16}SnO_2N_6S_2]$, E = $[C_{28}H_{18}CoO_6N_2].2H_2O$, F = $[C_{18}H_{22}CdO_2N_6S_2]$ and K = Kanamycin

4. CONCLUSIONS

In this paper we have explored the synthesis and coordination Chemistry of Ni(II), Zn(II), Mn(II), Sn(II), Co(II) and Cd(II) ions were synthesized with three different synthesized Schiff base ligands viz (L^1) [2-(2-hydroxybenzylidene) hydrazinecarbothioamide, (L^2) [4-((4-hydroxybenzylidene) amino)benzoic acid and (L^3) [2-(4-methoxybenzylidene)hydrazinecarbothioamide]. The ligands and metal complexes were characterized by molar conductivity measurement, magnetic susceptibility, Infrared, electronic spectral, thermal analysis and some physical measurements. The overall reactions were monitored by TLC analysis. Molar conductance study has shown that all the complexes were non-electrolytic in nature. FTIR studies suggested that Schiff bases act as deprotonated bidentate ligands and metal ions are attached with the ligands-(L^1), (L^2) by N, O and ligand-(L^3) by N, S coordinating sites during complexation reaction. Magnetic susceptibility data coupled with electronic spectra revealed that $[ZnC_{16}H_{16}O_2N_6S_2].2H_2O$, $[MnC_{16}H_{16}O_2N_6S_2].H_2O$, $[SnC_{16}H_{16}O_2N_6S_2]$ and $[CdC_{18}H_{22}O_2N_6S_2]$ complexes have tetrahedral, $[NiC_{16}H_{16}O_2N_6S_2].H_2O$ has a square planer and $[CoC_{28}H_{18}O_6N_2].2H_2O$ has octahedral geometry. Thermal analysis (TGA and DTG) data showed the possible degradation pathway of the complexes and also indicated that most of the complexes were thermally stable up to 200°C. The Schiff bases and their metal complexes have been found moderate to strong antimicrobial activity.

COMPETING INTERESTS

Authors have declared that no competing interests exist.

REFERENCES

1. Angela Kriza, Lucica Viorica Ababei, Nicoleta Cioatera, Ileana Rău And Nicolae Stănică, Synthesis And Structural Studies Of Complexes Of Cu, Co, Ni And Zn With Isonicotinic Acid Hydrazide And Isonicotinic Acid (1-Naphthylmethylene) Hydrazide, J. Serb. Chem. Soc. 2010; 75(2):229- 242.
2. Das PK, Panda N, Behera NK. Synthesis, characterization and antimicrobial activities of Schiff base complexes derived from isoniazid and Diacetyl monoxime. IJSET – Int. J. of Innovative Sci., Eng. & Tech. 2016;3(1):42-54.
3. Anil Kumar MR, Shanmukhappa S, Rangaswamy BE, Revanasiddappa M. Synthesis, characterization, antimicrobial activity, antifungal activity and dna cleavage studies of transition metal complexes with Schiff base Ligand. Int. J. of Innovative Sci., Eng. & Tech. 2015;4(2): 60-66.
4. O' Boyle NM, Tenderholt AL, Langer KM. Cclib: A library for package-independent computational chemistry algorithms J. Comput. Chem. 2008;29:839.
5. Saud I. Al-Resayes, Mohammad Shakir, Ambreen Abbasi, Kr. Mohammad Yusuf Amin, Abdul Lateef. Synthesis, spectroscopic characterization and biological activities of N4O2 Schiff base ligand and its metal complexes of Co(II), Ni(II), Cu(II) and Zn(II), Spectromica Acta Part A. 2012;93:86-94.
6. Karlin KD, Tyeklar Z. Bioinorganic chemistry of copper. Chapman & Hall: New York. 1993;101-109.
7. Arun V, Sridevi N, Robinson PP, Manju S, Yusuff KKM. Ni(II) and Ru(II) Schiff base

- complexes as catalysts for the reduction of benzene. *J. Mol. Catal. A: Chem.* 2009; 304(1-2):191-198.
8. Gupta KC, Sutar AK. Catalytic activities of Schiff base transition metal complexes, *Coord. Chem. Rev.* 2008;252(12-14): 1420-1450.
 9. Kureshy RI, Khan NH, Abdi SHR, Iyer P, Patel ST. Chiral Ru(II) Schiff base complexes catalysed enantio selective epoxidation of styrene derivatives using iodosyl benzene as oxidant II. *J. Mol. Catal.* 1999;150(1-2):175-183.
 10. Saud I. Al-Resayes, Mohammad Shakirb, Ambreen Abbasi, Kr. Mohammad Yusuf Amin, Abdul Lateef, *Spectromica Act. A Part A.* 2012;93:86-94.
 11. Rakesh Ranjan, Dhanashree S Hallooman. Synthesis and Characterization of Co(II) and Ni(II) Complexes with Schiff Base 2,2-Dimethylpropiophenonethiosemicarbazone, *Int. J. of Res. In Pharm. And Chem.* 2014; 4(2):423-426.
 12. Angela Kriza, Mariana Loredana Dianu, Nicolae Stănică, Constantin Drăghici, Mona Popoiu. Synthesis and Characterization of Some Transition Metals Complexes with Glyoxalbis-Isonicotinoyl Hydrazone. 2009;60(6):555-560.
 13. Mitu L, Kriza A. Synthesis and characterization of complexes of Mn(II), Co(II), Ni(II) and Cu(II) with an Aroylhydrazone Ligand. *Asian J. Chem.* 2007;19(1):658-664.
 14. Ljubijankić N, Tešević V, Grgurić-Šipka S, Jadranin M, Begić S, Buljubašić L, Markotić E, Ljubijankić S. Synthesis and characterization of Ru(III) complexes with thiosemicarbazide-based ligands. 2016;47: 1-6.
 15. Methak S. Mohammad. Preparation and characterization of some transition metal complexes with Schiff base of thiosemicarbazone. *J. of Kerbala Uni. Scien.* 2010;8(1):8-17.
 16. Singh RV, Fahmi N, Biyala MK. Coordination behavior and biopotency of N and S/O donor ligands with their palladium(II) and platinum(II) complexes. *J. of the Ir. Chem. Soc.* 2005;2(1):40-46.
 17. Vijey M, Shiny G, Vaidhyalingam V. Synthesis and antimicrobial activities of 1-(5-substituted-2-oxo indolin-3-ylidene)-4-(substituted pyridin-2-yl) thiosemicarbazide, *Arkivoc* (xi). 2008;187.
 18. Mohammad Asif. A review on biological activities of benzimidazole, oxadiazole and mannich base derivatives of benzimidazole-oxadiazole merged compounds. *Int. J. of Cur. Res. in App. Chem. & Chem. Eng.* 2017;3(1):20-29.
 19. Khalil MMH, Aboaly MM, Ramadan RM. Spectroscopic and electrochemical studies of ruthenium and osmium complexes of salicylideneimine-2-thiophenol Schiff base, *Spectrochimica Acta Part A: Mol. and Bio. Spec.* 2005;61(1):157-161.
 20. Dahikar PM, Kedar RM. Synthesis spectral and biological activity of transition metal complexes of substituted benzoinsemi-carbazones. *Inter. J. of Appl. or Inn. In Engg. & Man. (IJAEM).* 2013;2(4):8-11.
 21. Murali Krishna P, Shankara BS, Shashidhar Reddy N. Synthesis, characterization, and biological studies of binuclear copper(II) Complexes of (2E)-2-(2-Hydroxy-3-Methoxybenzylidene)-4N-Substituted Hydrazine carbothioamides, Hindawi Publishing Corporation, International Journal of Inorganic Chemistry. 2013;11.
 22. Ljiljana S, Vojinović-Ješić, Vukadin M, Leovac Mirjana M, Lalović Valerija I, Češljević Ljiljana S, Jovanović Marko V. Rodić, Vladimir Divjaković. Transition metal complexes with thiosemicarbazide-based ligands. Part 58. Synthesis, spectral and structural characterization of dioxovanadium(V) complexes with Salicylaldehydethiosemicarbazone, *J. Serb. Chem. Soc.* 2011;76 (6):865–877.
 23. Monika Tyagi, Sulekh Chandra. Synthesis, characterization and biocidal properties of platinum metal complexes derived from 2,6-diacetylpyridine (bisthiosemicarbazone), *Open Jo. of Inorg. Chem.* 2012;2:41-48.
 24. Vojinović-JešićL JS, Leovac VM, Lalović MM, Češljević VI, Jovanović LJS, Rodić MV, Divjaković V. Transition metal complexes with thiosemicarbazide-based ligands. Part 58. Synthesis, spectral and structural characterization of dioxovanadium(V) complexes with salicyl aldehyde thiosemicarbazone, *J. Serb. Chem. Soc.* 2011;76 (6):865–877.
 25. Baiu SH, El-Ajaily MM, El-Barasi, Antibacterial activity of Schiff base

- Chelates of divalent metal ions. Asian Journal of Chemistry. 2009;21(1):5-10.
26. Elena Pahontu, Valeriu Fala, Aurelian Gulea, Donald Poirier, Victor Tapcov, Tudor Rosu. Synthesis and characterization of some new Cu(II), Ni(II) and Zn(II) complexes with salicylidene thiosemicarbazones: Antibacterial, antifungal and *in vitro* antileukemia activity, *Molecules*. 2013;18:8812-8836.
 27. El-Bahnasawy RM, Sharaf El-Deen LM, El-Table AS, Wahba MA, El-Monsef A. Electrical conductivity of salicylaldehyde thiosemicarbazone and its Pd(II), Cu(II) and Ru(III) complexes. *Eur. Chem. Bull*, 2014;3(5):441-446.
 28. Md. Saddam Hossain, Zakaria CM, Haque MM, Md. Kudrat E. Zahan. Spectral and thermal characterization with antimicrobial activity on Cr(III) and Sn(II) complexes containing N,O Donor novel schiff base ligand, *Int. J. of Chem. Studies*. 2016; 4(6):08-11.
 29. Xavier P. Gopu, Akila B, Suganya K. Synthesis and characterization of Schiff base from 3, 5-Di chloro salicylaldehyde with 4-bromoaniline and 4-aminobenzoic acid and its 1st row transition metal complexes. *Int. J. of Inn. Res. & Dev*. 2015;4(8):384-396 .
 30. Manohar V. Lokhande, Mrityunjay R. Choudhary, some transitional metal ions complexes with 3-[(E)-(4-Fluorophenyl) Methylidene] amino} benzoic acid and its microbial activity. *International Journal of Pharmaceutical Sciences and Research*. IJPSR. 2014;5(5):1757-1766.
 31. Gopu P, Xavier A. Synthesis and characterization of 4-(3-bromo-5 -chloro-2-hydroxybenzlidimino) benzoic acid and its transition metal complexes. *International Journal of Science and Research (IJSR)*. 2015;4(8):15-21.
 32. Shanker K, Rohini R, Ravinder V, Reddy PM. Ru(II) complexes of N₄ and N₂O₂ macrocyclic Schiff base ligands: Their antibacterial and antifungal studies. *Spectro Chimica Acta A*. 2009;73:1205-211.
 33. Raju Ashokan, Saravanan Sathishkumar, Ekamparam akila and rangappan rajavel, synthesis, characterization and biological activity of Schiff base metal complexes derived from 2, 4-dihydroxyacetophenone. *Chemical Science Transactions*. 2017; 6(2):277-287.
 34. Miguel-Angel Munoz-Hernandes, Michal L. Mckee, Timothy S. Keizer, Burt C. Yearwood and david atwood, six-coordinate aluminiumcations: Characterization, catalysis, and theory. 2002;3.
 35. Nakamoto K. Infrared spectra of inorganic and coordination compounds. John Wiley & Sons, New York, 2nd Edition; 1970.
 36. Shanker KB, Rohini M, Ravinder Reddy P, Ho MYP. Synthesis of tetraaza macrocyclic Pd(II) complexes; antibacterial & catalytic studies. *J. of the Ind. Chem. Soc*. 2009;86.
 37. Satheesh KP, Suryanarayana Rao V. Spectrophotometric method for the determination of trace amount of tungsten (Vi) in alloy samples using 4-hydroxy benzaldehyde thiosemicarbazone. *J. of Adv. Scien. Res*. 2015;6(2):14-17.
 38. Janarthanan S, Rajan YC, Umarani PR, Jayaraman D, Premanand D, Pandi S. Synthesis, growth, optical and thermal properties of a new organic crystal semicarbazone of p-anisaldehyde (SPAS). 2010;3(8):42-47.
 39. Ruchi Agarwal, Mohd. Asif Khan, Shamim Ahmad. Schiff base complexes derived from thiosemicarbazone, synthesis characterization and their biological activity. *Journal of Chemical and Pharmaceutical Research*. 2013;5(10):240-245.
 40. Sandra S. Konstantinovi, Blaga C. Radovanovi, Ivojin Caki, Vesna Vasi. Synthesis and characterization of Co(II), Ni(II), Cu(II) and Zn(II) complexes with 3-salicylidenehydrazono-2-indolinone. *J. Serb. Chem. Soc*. 2003;68(8-9):641-647.
 41. Gondia NK, Priya J, Sharma SK. Synthesis and physico-chemical characterization of a Schiff base and its zinc complex. *Res Chem Intermed*. 2017;43:1165-1178.
 42. Lotf A. Saghatforoush, Ali Aminkhani, Sohrab Ershad, Ghasem Karimnezhad, Shahriar Ghammamy, Roya Kabiri. Preparation of zinc (II) and cadmium (II) complexes of the tetradentate Schiff base ligand 2-((E)-(2-(2(pyridine-2-yl)-ethylthio) ethylimino)methyl)-4-bromophenol (Pyt Brsal H). *Molecules*. 2008;13:804-811.

43. Jian-Ning Liu, Bo-Wan Wu, Bing Zhang, Yongchun Liu. Synthesis and characterization of metal complexes of Cu(II), Ni(II), Zn(II), Co(II), Mn(II) and Cd(II) with tetradentate Schiff bases. *Turk J Chem.* 2006;30:41-48.
44. Shayma A. Shaker, Preparation and Spectral Properties of Mixed-Ligand Complexes of VO(IV), Ni(II), Zn(II), Pd(II), Cd(II) and Pb(II) with Dimethylglyoxime and N-Acetylglycine, *E-Journal of Chemistry.* 2010;7(S1):S580-S586.
45. Md. Kudrat E Zahan, Islam MS, Md. Abul Bashar. Synthesis, characteristics, and antimicrobial activity of some complexes of Mn(II), Fe(III) Co(II), Ni(II), Cu(II), and Sb(III) containing bidentate Schiff base of SMDTC. *Russian Journal of General Chemistry.* 2015;85(3):667–672.
46. Rehab K. Al-Shemary, Ahmed T. Numan, Eman Mutar Atiyah. Synthesis, characterization and antimicrobial evaluation of mixed ligand complexes of manganese(II), cobalt(II), copper(II), nickel(II) and mercury(II) with 1,10-phenanthroline and a bidentate Schiff base. *Eur. Chem. Bull.*, 2016;5(8):335-338.
47. Iniyama GE, Olarele OS, Johnson A. Synthesis, spectral, characterization and antimicrobial activity of manganese (II) and copper (II) complexes of Salicylaldehydephenylhydrazone. *Int. J. of Chem. and Appl.* 2015;7(1):15-23.
48. Neelofar, Nauman Ali, Shabir Ahmad, Naser M. Abdel-Salam, Riaz Ullah, Robila Nawaz, Sohail Ahmad. Synthesis and evaluation of antioxidant and antimicrobial activities of Schiff base tin (II) complexes. *Tropical Journal of Pharmaceutical Research.* 2016;15(12):2693-2700.
49. Har Lal Singh, Singh JB. Synthesis and characterization of new lead(II) and organotin(IV) complexes of Schiff bases derived from histidine and methionine, hindawi publishing corporation. *International Journal of Inorganic Chemistry.* 2012;7.
50. Sunita Bhanuka, Har Lal Singh. Spectral, dft and antibacterial studies of tin(II) complexes of Schiff bases derived from aromatic aldehyde and amino acids. *Rasayan J. Chem.* 2017;10(2):673-68.
51. Khalil Abid, Sinann Al-Bayati, Anaam Rasheed. Synthesis, characterization, thermal study and biological evaluation of transition metal complexes supported by onno-pentadentate Schiff base ligand. *American Journal of Chemistry.* 2016; 6(1):1-7.
52. Allan JR, Veitch PM. The preparation, characterization and thermal analysis studies on complexes of cobalt(II) with 2-, 3-, 4-cyanopyridines. *J. Thermal Anal.* 1983;27(1):3-15.
53. Moamen S. Refat, El-Deen IM, El-Garib MS, Abd El-Fattah W. Spectroscopic and anticancer studies on new synthesized copper(II) and manganese(II) complexes with 1,2,4- triazines thiosemicarbazide1. *Russian J. of Gen. Chem.* 2015;85(3): 692–707.
54. Md. Saddam Hossain, Md. Ashraful Islam, Zakaria CM, Haque MM, Md. Abdul Mannan, Md. Kudrat-E-Zahan. Synthesis, spectral and thermal characterization with antimicrobial studies on Mn(II), Fe(II), Co(II) and Sn(II) complexes of tridentate N,O coordinating novel Schiff base ligand. *J. Chem. Bio. Phy. Sci. Sec. A.* 2016; 6(1):041-052.
55. Islam MR, Shampa JA, Kudrat E Zahan M, Haque MM, Reza Y. Investigation on spectroscopic, thermal and antimicrobial activity of newly synthesized binuclear Cr(III) metal ion complex. *J. Sci. Res.* 2016;8 (2):181-189.
56. Sayed M. Abdallah MA. Zayed, Gehad G. Mohamed. Synthesis and spectroscopic characterization of new tetradentate Schiff base and its coordination compounds of non donor atoms and their antibacterial and antifungal activity. *Arabian J. of Chem.* 2010;3:103–113.
57. Samir Alghool. Mononuclear complexes based on reduced Schiff base derived from L-methionine, synthesis, characterization, thermal and *in vitro* antimicrobial studies. *J Therm Anal Calorim.* 2015;12: 1309–1319.
58. Achut S. Munde, Amarnath N. Jagdale, Sarika M. Jadhav, Trimbak K. Chondhekar. Synthesis, characterization and thermal study of some transition metal complexes of an asymmetrical tetradentate Schiff base ligand. *J. Serb. Chem. Soc.* 2010;75(3):349–359.

59. Munde AS, Shelke VA, Jadhav SM, Kirdant AS, Vaidya SR, Shankarwar SG, Chondhekar TK. Synthesis, characterization and antimicrobial activities of some transition metal complexes of biologically active asymmetrical tetradentate ligands. Adv. Appl. Sci. Res. 2012;3(1):175-182.

© 2018 Afsan et al.; This is an Open Access article distributed under the terms of the Creative Commons Attribution License (<http://creativecommons.org/licenses/by/4.0>), which permits unrestricted use, distribution, and reproduction in any medium, provided the original work is properly cited.

Peer-review history:

The peer review history for this paper can be accessed here:

<http://prh.sdiarticle3.com/review-history/24702>